Annual Report, 1998

Management of LARSE II (UCLA) Stress Modeling and Data Analysis

Paul Davis

The work performed over the last year falls into three categories:

- Estimation of southern California anisotropy and its relation to tectonics.
- Visualization of the past 16 M.yr. of California Tectonics for geophysical comparison.
- P-wave Amplitude variation from the Southern California Seismic Network.

Southern California Anisotropy

P. Davis, S. Baher, M. Kohler

Figure (1a) shows splitting results from the Los Angeles Basin Passive Seismic Array which was installed in 1997 and ran for nine months. These results are typical for the region (e.g. Liu et al., 1996). Splitting of SKS waves is observed at all seismic stations in southern California. The fast polarizations are directed east-west to north northeast-west southwest. Splitting is thought to occur in the uppermost mantle. A full description of the SCEC 3D Seismic Velocity Model should also include anisotropy. In order to constrain the depth extent of the anisotropy and its three dimensional tensor, other measures of anisotropy are required. Sung and Jackson (1992) and Hearn (1996) have measured anisotropy in Pn travel times. Polet and Kanamori (1997) have measured anisotropy in surface wave arrivals finding Love wave velocities higher than Rayleigh waves. We have carried out a detailed analysis of all SKS and SKKS at station PAS (Pasadena) and find that SKS splitting times and fast directions exhibit a sin(2z), cos(2z) variation, where z is azimuth. Combining all these different estimates we have inverted for values of the uppermost mantle elastic tensor C_{ijkl}. By restricting the anisotropy to be orthorhombic, consistent with the major mantle minerals, we reduce the number of degrees of freedom of the tensor from 21 independent values to twelve, 9 elastic constants, and three Euler angles. The resulting fit to the Pn, Rayleigh, Love and SKS splitting results are shown in figure (1b). Most constants are well determined. Those associated with anisotropy of vertically travelling P waves are the least constrained. The agreement between splitting, surface waves and Pn suggest that the anisotropy is developed in the uppermost mantle directly beneath the Moho. The fast directions are found to be nearly horizontal. If caused by fossil Farallon plate beneath southern California, its fabric is nearly horizontal, suggesting very shallow subduction. The alternative view, that it is due to finite strain, implies that the major mantle extension has been directed east-west, which is not incompatible with recent California transpressive tectonics. We are examining the strain history using palinspastic reconstructions based on geological data to test these alternatives.

California Paleo-Tectonics

(M. Jackson, C. Wood, R. Ingersoll, P. Davis)

The objective here is to visualize the last 16 M.yr. of California tectonics in order to relate the 3D structures seen by LARSE to the geological history. We believe that this is a necessary step in order to understand how stresses are applied and relieved. Ingersoll and Rumelhart (1999) have used sedimentary indicators to back - rotate and translate the California blocks lying between the major faults. We have taken those maps and digitized them (Figure 1) with the purpose of making a movie of the last 16 M.yr. of tectonic evolution for comparison with the geophysics. We fit current day topography to each segment using the newly available (30") DEM maps. Figure 2 shows 25 frames between 12 M.yr. and 0 M.yr. at 0.5 M.yr. time steps. To make the movie we assign topography to each segment and linearly interpolate between the maps at 0.5 M.yr. intervals. Overlapping segments correspond to regions that experience future extension. In particular the stacked segments of 16 M.yr. are related to reverse subduction which occurs associated with the rotation of the Transverse Ranges and exposure of the Catalina schist. This model favors a transition from a dilatational jog of the San Gabriel - Chrisianitos fault system, which forms the LA basin 12- 6 M.yr. to the compressional jog of the big bend of the San Andreas at 6-0 M.yr. While the details of the model are under revision by Ingersoll and Rumelhart, the structure is easily modified to include multiple layers using Arc Info vizualization. We anticipate including best estimates of paleo-variation in the topography (e.g. development of basins, mountains) and estimates of Moho, and sediment-basement interfaces.

P-wave Amplitude variation from the Southern California Seismic Network
(Possible application to Sherman Oaks Damage)
(D. Icenogle, P. Davis)

The objective is to determine how amplitude variation in southern California depends on structure and topography. This project has been supported in the past by the USGS. We briefly report overlap with our ongoing SCEC projects. Recognition of anomalous amplification, such as has been hypothesized to have caused the enhanced damage at Santa Monica and Sherman Oaks at the time of the Northridge earthquake, requires determination of a standard background - average amplification model. We use data from the SCEC data base at almost 200 stations of the southern California seismic network. We have begun our analysis using P waves. After correcting for instrument response, we measured maximum amplitudes within a 3 second window of the theoretical arrival of the P wave. We fit the amplitude pattern to a model consisting of the radiation pattern for the fault plane solution multiplied by a $1/r^m$ geometric attenuation. We have been surprised to find that $m = 0.3\pm0.1$ rather than 1.0, expected for spherical waves in afull-space, or 0.5 for cylindrical waves. We have experimented with a linear gradient in velocity but find that to match the amplitudes requires a non-linear gradient. We use the average amplification model to characterize P-wave amplification factors at individual stations by averaging ratios of observed amplitudes to theoretical ones. Figure (3) shows the distribution of amplification factors obtained from 70 earthquakes. We see that the highest amplifications correspond to the highest, and most rugged topography. We are compiling amplitude factors as a function of azimuth in order to recognize directional dependencies that might be explainable in terms of topographic strike or buried structures. The extreme damage from the Northridge earthquake at Sherman Oaks has not been satisfactorily explained. Damage in the lower regions is probably due to the LA river sediments and unconsolidated landfill. However it is not clear why there was more damage in the Sherman Oaks part of the Santa Monica Mountains than in the Encino part, which lies closer to the hypocenter. If the contrast is due to contrasting topography, we may be able to recognize what combinations of incident waveforms and relief are most hazardous.

Figure 1. SKS splitting measured on the Los Angeles Basin Passive Seismic Array. Splitting times are about 1.1 seconds. Lines give orientation of the fast direction.

Figure 2. Frames of tectonic evolution of Southern California at 0.5 million year intervals over the past 12 million years. In this version topography has not been varied from present day values. Note the emergence of Catalina I. as the transverse ranges rotate, the extension of the LA basin followed by contraction.

Figure 3. Average P-wave amplitudes as SCSN stations from 70 local earthquakes. High values occur in regions of elevated topography.

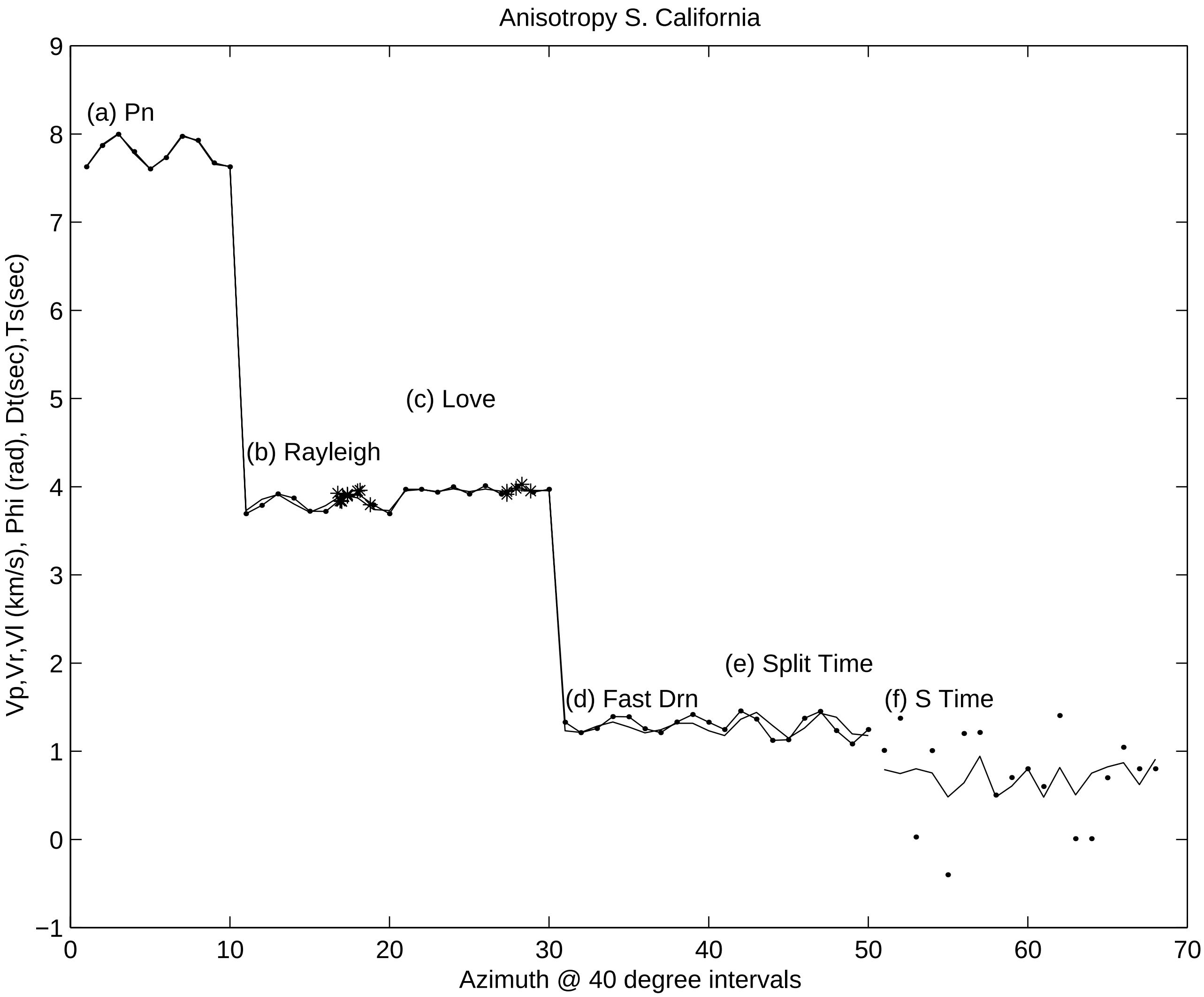

Anisotropy S. California
Vp,Vr,Vl (km/s), Phi (rad), Dt(sec),Ts(sec)
Azimuth @ 40 degree intervals
(a) Pn
(b) Rayleigh
(c) Love
(d) Fast Drn
(e) Split Time
(f) S Time
9
8
7
6
5
4
3
2
1
0
−1
0
10
20
30
40
50
60
70

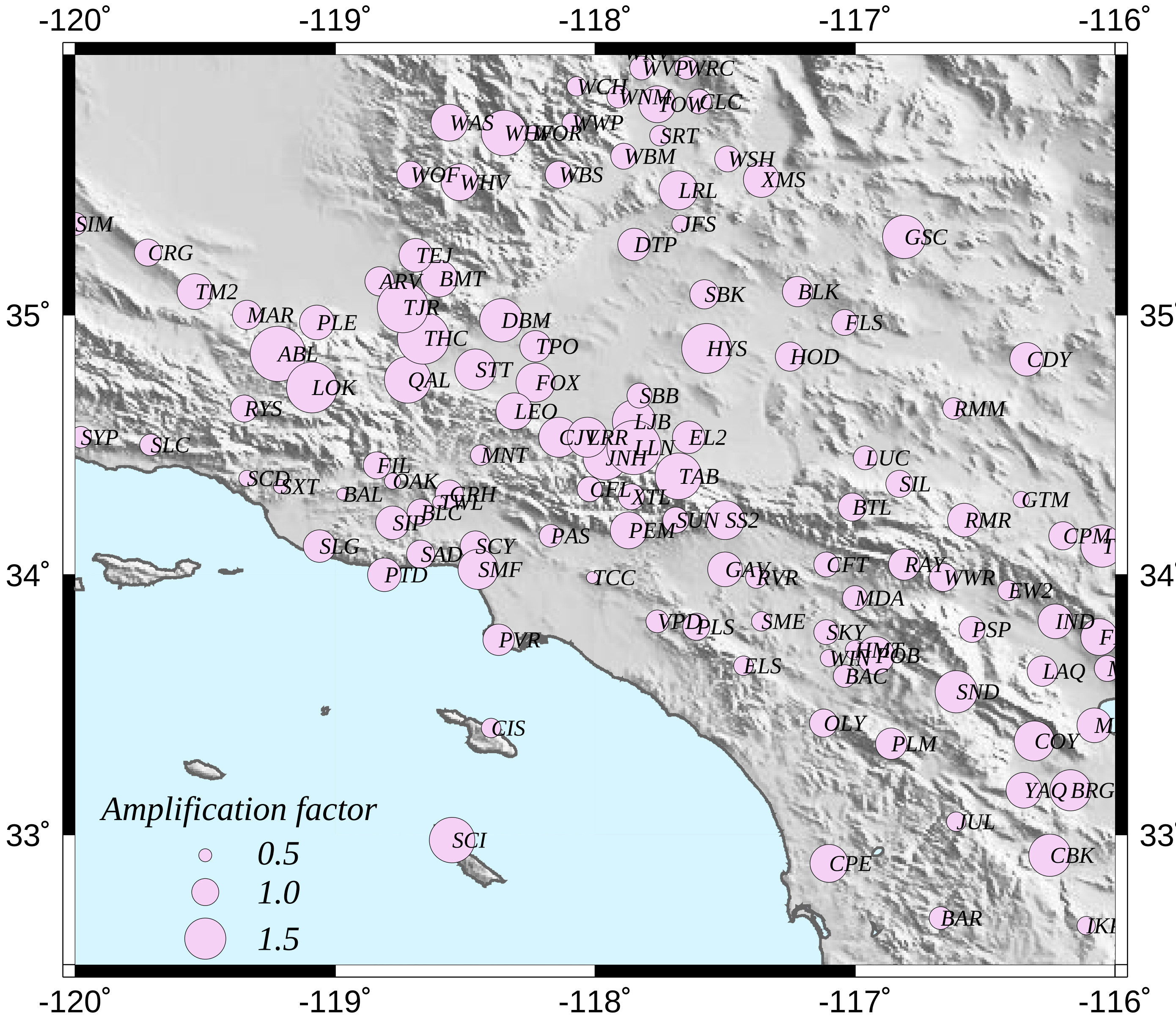

-120°
-119°
-118°
-117°
-116°
35°
34°
33°
WVP
PWRC
WCH
WNM
TOW
CLC
WAS
WHF
WOR
WWP
SRT
WBM
WSH
WOF
WHV
WBS
XMS
LRL
SIM
JFS
CRG
DTP
GSC
TEJ
ARV
BMT
TM2
SBK
BLK
MAR
TJR
PLE
DBM
FLS
ABL
THC
TPO
HYS
HOD
CDY
QAL
STT
LOK
FOX
SBB
RYS
LEO
RMM
LJB
SYP
SLC
CJV
LRR
EL2
LLN
MNT
JNH
LUC
FIL
SCD
OAK
TAB
SXT
BAL
CRH
CFL
XTL
SIL
GTM
TWL
BLC
BTL
SIP
SUN
SS2
RMR
PAS
PEM
CPM
SLG
SCY
SAD
GAV
RVR
CFT
RAY
SMF
WWR
PTD
TCC
EW2
MDA
VPD
PLS
SME
IND
SKY
PSP
PVR
HMT
PDB
WIN
ELS
BAC
LAQ
SND
CIS
OLY
PLM
COY
YAQ
BRG
JUL
SCI
CPE
CBK
BAR
Amplification factor
0.5
1.0
1.5